



Contents lists available at ScienceDirect

NeuroImage

journal homepage: www.elsevier.com/locate/ynimg

Different topological organization of human brain functional networks with eyes open versus eyes closed

Q1 Pengfei Xu^a, Ruiwang Huang^{a,b}, Jinhui Wang^a, Nicholas T. Van Dam^c, Teng Xie^a, Zhangye Dong^a,
4 Chunping Chen^d, Ruolei Gu^d, Yu-Feng Zang^{a,e}, Yong He^a, Jin Fan^{f,g,h,i}, Yuejia Luo^j.

^a State Key Laboratory of Cognitive Neuroscience and Learning, Beijing Normal University, Beijing 100875, China

^b Brain Imaging Center, Center for Studies of Psychological Application, Guangdong Key Laboratory of Mental Health and Cognitive Science, School of Psychology, South China Normal University, Guangzhou 510631, China

^c Department of Psychiatry, New York University School of Medicine, New York, NY 10016, USA

^d Key Laboratory of Mental Health, Institute of Psychology, Chinese Academy of Sciences, Beijing 100101, China

^e Center for Cognition and Brain Disorders, Affiliated Hospital, Hangzhou Normal University, Hangzhou 310015, China

^f Department of Psychology, Queens College, The City University of New York, New York, NY 11367, USA

^g Department of Psychiatry, Mount Sinai School of Medicine, New York, NY 10029, USA

^h Fishberg Department of Neuroscience, Mount Sinai School of Medicine, New York, NY 10029, USA

ⁱ Friedman Brain Institute, Mount Sinai School of Medicine, New York, NY 10029, USA

^j Institute of Affective and Social Neuroscience, Shenzhen University, Shenzhen 518060, China

ARTICLE INFO

Article history:

Accepted 30 December 2013

Available online xxx

Keywords:

Exteroceptive

Interoceptive

Connectome

Graph theory

Resting-state functional MRI

ABSTRACT

Opening and closing the eyes are a fundamental behavior for directing attention to the external versus internal 30 world. However, it remains unclear whether the states of eyes-open (EO) relative to eyes-closed (EC) are associ- 31 ated with different topological organizations of functional neural networks for exteroceptive and interoceptive 32 processing (processing the external world and internal state, respectively). Here, we used resting-state functional 33 magnetic resonance imaging and neural network analysis to investigate the topological properties of functional 34 networks of the human brain when the eyes were open versus closed. The brain networks exhibited increased 35 cliquishness and increased local efficiency, but lower global efficiency during the EO state. Together, these prop- 36 erties suggest an increase in specialized information processing along with a decrease in integrated information 37 processing in EO (vs. EC). More importantly, the “exteroceptive” network, including the attentional system (e.g., 38 superior parietal gyrus and inferior parietal lobule), ocular motor system (e.g., precentral gyrus and superior 39 frontal gyrus), and arousal system (e.g., insula and thalamus), showed higher regional nodal properties (nodal 40 degree, efficiency and betweenness centrality) in EO relative to EC. In contrast, the “interoceptive” network, com- 41 posed of visual system (e.g., lingual gyrus, fusiform gyrus and cuneus), auditory system (e.g., Heschl's gyurs), so- 42 matosensory system (e.g., postcentral gyrus), and part of the default mode network (e.g., angular gyrus and 43 anterior cingulate gyrus), showed significantly higher regional properties in EC vs. EO. In addition, the connec- 44 tions across sensory modalities were altered by volitional eye opening. The synchronicity among visual system 45 and motor, somatosensory and auditory system characteristics of EC was attenuated in EO, and the connections 46 among visual system and attention, arousal and subcortical systems were increased in EO. These results may in- 47 dicate that EO leads to a suppression of sensory modalities (other than visual) to allocate resources to exterocep- 48 tive processing. Our findings suggest that the topological organization of human brain networks dynamically 49 switches corresponding to the information processing modes as we open or close our eyes. 50

© 2014 The Authors. Published by Elsevier Inc. All rights reserved. 51

Introduction

While vision has featured centrally in prominent scientific theories 57 of consciousness (Crick and Koch, 2003), we spend a considerable por- 58 tion of our lives with our eyes closed, thereby attenuating the potential 59 contributions of vision. Interestingly, a recent study suggested that mo- 60 mentary closing of the eyes (blinking) not only occurs more often than 61 would be necessary for ocular lubrication, but that these blinks are asso- 62 ciated with subtle shifts in neural activity (Nakano et al., 2013). While 63 awake, awareness shifts based on whether our eyes are open or closed; 64

This is an open-access article distributed under the terms of the Creative Commons Attribution-NonCommercial-No Derivative Works License, which permits non-commercial use, distribution, and reproduction in any medium, provided the original author and source are credited.

Correspondence to: R. Huang, Centre for Studies of Psychological Application, Guangdong Key Laboratory of Mental Health and Cognitive Science, School of Psychology, South China Normal University, Guangzhou 510631, China. Fax: +86 20 8521 6499.

Corresponding author. Fax: +86 10 58802365.

E-mail addresses: ruiwang.huang@gmail.com (R. Huang), luoyj@bnu.edu.cn (Y. Luo).

1053-8119/\$ – see front matter © 2014 The Authors. Published by Elsevier Inc. All rights reserved.
<http://dx.doi.org/10.1016/j.neuroimage.2013.12.060>

Please cite this article as: Xu, P., et al., Different topological organization of human brain functional networks with eyes open versus eyes closed, NeuroImage (2014), <http://dx.doi.org/10.1016/j.neuroimage.2013.12.060>

awareness has been described as “exteroceptive” when the eyes are open (EO) and “interoceptive” when the eyes are closed (EC). These states correspond to focus on the “outside” versus the “inside”, respectively, and each has different psychophysiological characteristics and underlying brain mechanisms (Marx et al., 2003).

Compared to EC, an increased attentional load and raised level of arousal is present in EO (Hufner et al., 2009). The differences attributable to these states may have more to do with the simple processing of visual information; even in the darkness, where little to no visual input is present, these two states reveal distinct neural activation patterns (Hufner et al., 2009). Attentional and oculomotor systems (e.g., superior parietal gyrus and frontal eye fields) show activation in EO, while sensory systems (e.g., visual, auditory, and somatosensory) show activation in EC (Bianciardi et al., 2009; Hufner et al., 2008, 2009; Marx et al., 2003, 2004; McAvoy et al., 2008; Niven and Laughlin, 2008). These findings suggest two different states of mental activity: an “exteroceptive” state characterized by overt attention and ocular motor activity (during EO) and an “interoceptive” state characterized by imagination and multisensory activity (during EC) (Hufner et al., 2009; Marx et al., 2004). The corresponding differences of spontaneous neural activity between these two states have been characterized in previous resting-state functional magnetic resonance imaging (R-fMRI) studies (Bianciardi et al., 2009; McAvoy et al., 2008; Yan et al., 2009; Yang et al., 2007; Zou et al., 2009).

More recently, an R-fMRI study manipulated both eyes open/closed and lights on/off. In this study, there were significant differences between EO and EC in both spontaneous brain activity and functional connectivity but no differences in whole brain topological organization other than connection distance (i.e., the Euclidean distance between each pair of regional nodes) (Jao et al., 2013). Given that the topological properties of human brain networks have shown correlations with various cognitive functions and pathologies (Bullmore and Sporns, 2009; He and Evans, 2010), it is curious that there were widespread influences of EO and EC on the spontaneous activity and connectivity but not on the topological organization of the networks (Jao et al., 2013).

Given that there are critical influence of different acquisition parameters and analytic strategies in R-fMRI data but lacking consensus about the best way to deal with it (Murphy et al., 2009; Wang et al., 2009; Wig et al., 2011; Zuo et al., 2013), we acquired human R-fMRI data and constructed whole brain functional networks with different brain parcellation templates and presence/absence of global signal regression (GSR) to compare topological parameters (e.g., small-world, network efficiency and nodal efficiency) of brain networks between the EO and EC states. We hypothesized that the “exteroceptive” state and the “interoceptive” state were associated with different topological organizations of brain networks corresponding to different information processing modes. Specifically, we predicted that there would be an “exteroceptive” network, characterized by attention and ocular motor system during EO, and an “interoceptive” network characterized by imagination and multisensory system during EC.

Materials and methods

Subjects

Twenty-three right-handed healthy volunteers (11 females; mean age \pm SD, 20.17 \pm 2.74 years) participated in this study. All participants were undergraduate/graduate students and had no history of neurological and psychiatric disorders or head injury. Written informed consent was obtained from each participant prior to the MRI acquisition. The study was approved by the Institutional Review Board of Beijing Normal University.

Data acquisition

MRI data were acquired on a Siemens Trio 3 T MRI scanner powered with a total imaging matrix technique at the Imaging Center for Brain

Research, at Beijing Normal University. Both the R-fMRI and high resolution 3D structural brain data were obtained using a 12-channel phased-array receiver-only head coil with the implementation of parallel imaging scheme GRAPPA (GeneRALized Autocalibrating Partially Parallel Acquisitions) (Griswold et al., 2002). For scanning, we selected the acceleration factor 2. The R-fMRI data were acquired using gradient-echo echo-planar imaging (EPI). The sequence parameters were as follows: TR = 3000 ms, TE = 30 ms, slice thickness = 3.5 mm with no gap, flip angle = 90°, FOV = 224 mm \times 224 mm, data matrix = 64 \times 64, interleaved 40 transversal slices giving spatial coverage 140 mm and 160 volumes. Each subject underwent the R-fMRI scans in two runs, EC state and EO state, each lasting 8 min. The order of the R-fMRI data acquisitions (corresponding to the two states) was counterbalanced across all subjects. In addition, we also acquired the 3D high-resolution brain structural images (1 mm³ isotropic) for each subject using a T1-weighted MP-RAGE sequence. The sequence parameters were TR/TE = 1900 ms/3.44 ms, flip angle = 9°, data matrix = 256 \times 256, FOV = 256 mm \times 256 mm, BW = 190 Hz/pixel, and 176 images along sagittal orientation, obtained in about 6 min.

Data preprocessing

The data preprocessing was conducted using SPM8 (<http://www.fil.ion.ucl.ac.uk/spm/>) and DPARSF (Yan and Zang, 2010). For each subject, the two R-fMRI runs (EO and EC) were processed separately. For each run, the first 10 volumes were discarded to account for the MR signal equilibration. The remaining functional images were first corrected for timing, and then realigned to the first volume to correct for head motion, which did not exceed 2.0 mm of displacement or 2.0° of rotation in any direction, in any subject. To account for the influence of head motion on R-fMRI (Mowinckel et al., 2012; Power et al., 2012; Satterthwaite et al., 2012; Van Dijk et al., 2012), the root mean squares of both overall head displacement and head rotation were calculated under EO and EC, and no significant differences were found between EO and EC ($p > 0.2$). Subsequently, the functional images were spatially normalized to the standard MNI-152 template and re-sampled to a voxel size of 3 \times 3 \times 3 mm³. The waveform of each voxel was finally passed through a band-pass filter (0.01–0.08 Hz) to reduce the effects of low-frequency drift and high-frequency physiological noise.

Construction of brain functional networks

The functional connectivity matrix of each subject was constructed based on the automated anatomical labeling (AAL) (Tzourio-Mazoyer et al., 2002), which parcellated the brain into 90 regions of interest (ROIs; Table S1). The mean time series of each ROI was calculated by averaging the time series of all voxels within that ROI. The effects of head-motion profiles and global signal were regressed out with multiple linear regression analyses as described in previous studies (Fox et al., 2005; Van Dijk et al., 2012; Wang et al., 2009). Given that the impact of global signal regression (GSR) is important and its contributions, intensely debated (Chai et al., 2012b; Fox et al., 2009; Murphy et al., 2009; Van Dijk et al., 2010; Weissenbacher et al., 2009), we repeated the data analysis without GSR to check the reliability of the results (Supplementary materials). Regression residuals were then substituted for the raw mean time series of the corresponding ROIs. Pearson's correlation between the residual time series of each pair of the 90 ROIs was calculated to obtain a symmetric correlation matrix, the functional connectivity matrix for each subject. Finally, all elements of the correlation matrix were truncated and binarized by using a pre-selected value of sparsity (the ratio between total number of edges and the maximum possible number of edges in a network). To ensure that the brain networks under EO and EC had the same number of edges, each correlation matrix was set to different thresholds over a specific range of sparsity (see the Results section), where prominent small-world properties in brain networks were observed (Watts and Strogatz, 1998b). For each

188 given sparsity, we obtained an undirected binarized network, in which
189 nodes represented brain regions and edges represented links between
190 brain regions. Graph theory was then applied to analyze the topological
191 organization of functional brain networks.

192 Network analysis

193 Global properties of functional brain networks

194 Graph theory can be used to characterize the brain functional net-
195 works quantitatively (Bullmore and Sporns, 2009; Hagmann et al.,
196 2008; He and Evans, 2010). Here, six network parameters: clustering
197 coefficient (C_p), characteristic path length (L_p), normalized clustering
198 coefficient (γ), normalized shortest path length (λ), global efficiency
199 (E_{glob}), and local efficiency (E_{loc}), were used to characterize the global
200 topological properties of brain networks. The definitions and descrip-
201 tions of C_p (Watts and Strogatz, 1998b), L_p (Newman, 2003), E_{glob}
202 (Latora and Marchiori, 2001), and E_{loc} (Latora and Marchiori, 2001)
203 can be found in the Appendix and in Rubinov and Sporns (2010).

204 The small-world property of a network can be characterized by both
205 the normalized clustering coefficient $\gamma = \frac{C_p^{real}}{C_p^{rand}}$ and the normalized charac-
206 teristic path length $\lambda = \frac{L_p^{real}}{L_p^{rand}}$ (Watts and Strogatz, 1998b). C_p^{real} and L_p^{rand}
207 are the clustering coefficient and the characteristic path length of the
208 real brain networks, and the C_p^{rand} and L_p^{rand} represent the mean indices
209 derived from matched random networks (100 matched random
210 networks were selected). The benchmark random networks were
211 constructed in a way that preserved the same number of nodes, edges,
212 and degree distribution as the real brain networks (Maslov and
213 Sneppen, 2002; Milo et al., 2002). Considering that correlation networks
214 are inherently more clustered than the nodes and degree matched ran-
215 dom networks, the Hirschberger-Qi-Steuer algorithm (H-Q-S; Zalesky
216 et al., 2012) was performed to verify the results. Typically, a small-
217 world network should meet the following criteria: $\gamma > 1$ and $\lambda \approx 1$
218 (Watts and Strogatz, 1998b), or $\sigma = \frac{\gamma}{\lambda} > 1$ (Humphries et al., 2006).

219 Regional properties of functional brain networks

220 In this study, three nodal parameters, degree (D) (Sporns and Zwi,
221 2004), nodal efficiency (E_{nod}) (Achard and Bullmore, 2007), and be-
222 tweenness centrality (BC) (Freeman, 1977), were adopted to character-
223 ize the regional properties of the functional networks. Their definitions
224 and descriptions are listed in Table A in the Appendix (see also Rubinov
225 and Sporns, 2010). The nodal characteristics of the brain networks mea-
226 sure the extent to which a given node connects to all other nodes of a
227 network and may indicate the importance of specific brain areas in
228 the network (Achard and Bullmore, 2007; He et al., 2008).

229 Integrated network parameters

230 In order to compare condition-related differences of topological
231 properties between brain functional networks regardless of the selec-
232 tion of specific thresholds, we calculated the integrated global param-
233 eters of the networks and the integrated regional nodal parameters of
234 node i as summations (Tian et al., 2011) (Table A). These integrated re-
235 gional nodal parameters were used to identify network hubs and to per-
236 form further statistical analyses.

237 Hub identification

238 Hubs refer to highly connected nodes in a network. In order to deter-
239 mine the hubs in the functional networks, we first calculated the nor-
240 malized nodal parameter for each node (Table A), then we identified
241 node i as a hub if any of its three nodal parameters $NS_{nod}(i)$ satisfied
242 the criteria (Table A). According to the above description, we deter-
243 mined the hubs of the functional neural networks corresponding to
244 EO and EC, respectively.

Statistical analysis

Network parameters

245 The integrated network parameters were used for t statistical com-
246 parison. Paired t -tests were performed to detect significant differences
247 for any of the six global network parameters ($p < 0.05$) or the three re-
248 gional nodal parameters ($p < 0.05$, uncorrected) between the EO and EC
249 states.
250
251

Inter-regional functional connectivity

252 To localize the specific connections altered by EO and EC, inter-
253 regional functional connectivity analysis was conducted. To control for
254 the family-wise error rate, we applied a network-based statistic method
255 (NBS; Zalesky et al., 2010a) for the connectivity matrices. A primary
256 cluster-defined threshold ($p = 0.001$) was used to define a set of
257 supra-threshold connections among which any connected component
258 and its size (number of links) were determined. To estimate the signifi-
259 cance for each component, we empirically derived the null distribution
260 of connected component size using a nonparametric permutation ap-
261 proach (1000 permutations). For each permutation, the two states (EO
262 and EC) were randomly re-allocated within each subject and a one-
263 tailed, paired t -test was computed independently for each link. Then
264 the same primary threshold ($p = 0.001$) was used to generate supra-
265 threshold links, among which the maximal connected component size
266 was recorded. Finally, for a connected component of size M found in
267 EO/EC, the corrected p -value was determined by finding the proportion
268 of the 1000 permutations for which the maximal connected component
269 was larger than M .
270

Results

Global properties of the functional brain networks

271
272 Fig. 1 shows the changes of topological parameters over a wide
273 range of sparsity (0.10–0.28) for the brain functional networks corre-
274 sponding to EO and EC. Because topological properties of the obtained
275 networks are affected by the choice of a specific sparsity value, setting
276 a specific sparsity as the threshold can ensure that the networks corre-
277 sponding to each subject have the same number of edges. To balance the
278 prominent small-world attribute and the appropriate sparseness in
279 brain functional networks across subjects, we set a series of threshold
280 values for sparsity in the range of 0.10–0.28 at an interval of 0.01. This
281 range of sparsity allows prominent small-world properties in brain net-
282 works to be observed (Watts and Strogatz, 1998a).
283

284 With the increase of sparsity, both the values of γ and λ decreased
285 monotonically. However, γ is much greater than 1 (Fig. 1C) whereas λ
286 approaches 1 (Fig. 1D) in brain functional networks under EO and EC
287 states. According to Watts and Strogatz (1998b), both of the two sets
288 of networks exhibited small-worldness ($\gamma > 1$ and $\lambda \approx 1$) in the
289 range of $0.10 \leq \text{sparsity} \leq 0.28$. In the present study, we considered
290 only the functional networks in $0.10 \leq \text{sparsity} \leq 0.28$ due to their
291 prominent small-worldness. The network efficiency analysis also dem-

292 onstrated the small-world configurations ($\frac{C_p^{real}}{C_p^{rand}} > 1$ and $\frac{L_p^{real}}{L_p^{rand}} \approx 1$, Figs. 1G
293 and H) in brain functional networks under EO and EC states.

294 Fig. 2 shows the integrated global parameters of the functional net-
295 works under the EO and EC states. Paired t -tests revealed significant dif-
296 ferences on the integrated global network parameters (C_p , λ , E_{loc} and
297 E_{glob}) between EO and EC ($p < 0.05$, Table 1). Compared to EC, the func-
298 tional networks under EO showed significantly greater C_p ($t = 3.79$,
299 $p < 0.01$, Figs. 1A and 2), λ ($t = 2.54$, $p < 0.02$, Figs. 1D and 2), and
300 E_{loc} ($t = 4.11$, $p < 0.01$, Figs. 1E and 2), but significantly smaller E_{glob}
301 ($t = -2.10$, $p < 0.05$, Figs. 1F and 2). No significant differences be-
302 tween the two states were found on L_p ($t = 1.95$, $p = 0.06$, Figs. 1B
303 and 2) or γ ($t = 0.37$, $p = 0.71$, Figs. 1C and 2). Given that correlation
304 networks are inherently more clustered than the node and degree

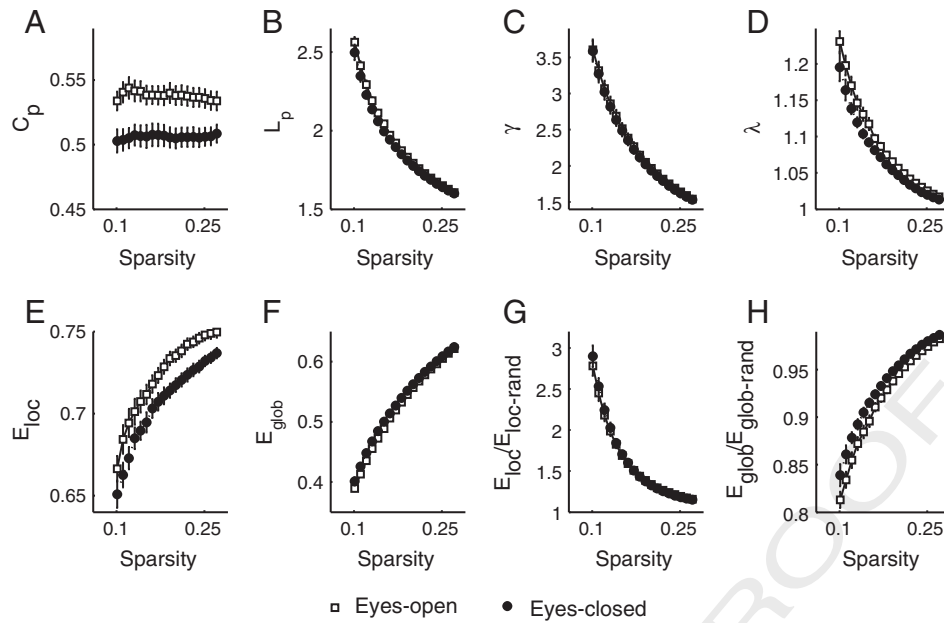


Fig. 1. Topological parameters of the human brain functional networks under eyes-open and eyes-closed changing with the sparsity. The square and circle correspond to the mean value of eyes-open and eyes-closed, respectively, and error bars to the standard error of the subject group in each state. At a wide range of sparsity (0.10–0.28), both of the networks showed $\gamma > 1$ and $\lambda \approx 1$, $E_{loc}/E_{loc-rand} > 1$, and $E_{glob}/E_{glob-rand} \approx 1$, which implies that the functional networks exhibit small-world properties. Abbreviations: C_p , clustering coefficient; L_p , characteristic path length; γ , normalized clustering coefficient; λ , normalized shortest path length; E_{loc} , local efficiency; E_{glob} , global efficiency.

matched random networks, the H–Q–S algorithm revealed that the differences between eyes-open and eyes-closed on γ was significant ($t = 3.77, p < 0.01$) but differences in λ were not significant ($t = 1.21, p = 0.24$).

Regional properties of the functional brain networks

Hub regions

Based on the three regional nodal parameters, D, E_{nod} , and BC , we found ten common hubs shared in functional networks corresponding to both EO and EC. These common hubs mainly include regions belonging to the arousal system (bilateral insula (INS), bilateral rolandic operculum (ROL), and right thalamus (THA.R) (Critchley, 2004; Critchley et al., 2011)), and motor system (right precentral gyrus (PreCG.R) and right supplementary motor area (SMA.R)) (Rizzolatti and Luppino, 2001), somatosensory system (right postcentral gyrus (PoCG.R)) (Fox et al., 1987), and other regions such as bilateral superior temporal

gyrus (STG) (Fig. 3A; Table S2). These ten common hubs for EO and EC are indicated by green spheres. In addition, twelve hubs specific to the functional networks of EO were detected, represented by the red color spheres in Fig. 3A. These hub regions were mainly located in regions related to the oculomotor system (PreCG.L) (Nobre et al., 1997), attentional system (left superior parietal gyrus (SPG.L), left inferior parietal lobule (IPL.L)) (Fan et al., 2005), arousal system (THA.L) (Critchley, 2004), and other regions such as bilateral supramarginal gyrus (SMG), bilateral opercular inferior frontal gyrus (IFGoperc), left medial superior frontal gyrus (SFGmed.L), left middle temporal gyrus (MTG.L), right inferior temporal gyrus (ITG.R), and right inferior orbitofrontal cortex (ORBinf.R). We also identified eleven hubs specific to the functional networks of EC, which are shown as blue color spheres in Fig. 3B (Table S2). These eleven hubs were mainly located in the visual system (left lingual gyrus (LING.L), right fusiform gyrus (FFG.R)) (Van Essen, 1979), somatosensory system (PoCG.L) (Fox et al., 1987), part of the default mode network (bilateral anterior cingulate gyrus (ACG), and right angular gyrus (ANG.R)) (Raichle et al., 2001; Van Dijk et al., 2010), and other regions such as bilateral superior temporal pole (TPOsup), bilateral middle frontal gyrus (MFG), right caudate (CAU.R).

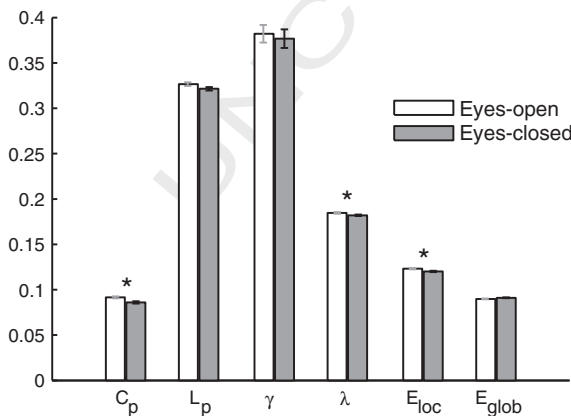


Fig. 2. Integrated global parameters of the brain functional networks corresponding to eyes-open (EO) and eye-closed (EC). Compared to EC, the values of C_p ($p = 0.001$), λ ($p = 0.019$), and E_{loc} ($p = 0.000$) were significantly higher, while the value of E_{glob} ($p = 0.048$) was significantly lower in EO. The symbol "*" indicates a significant difference in the global parameter between the two states.

Table 1

Significant differences in integrated global network parameters between eyes-open and eyes-closed revealed by the paired t -test.

	Eyes open	Eyes closed	Eyes open–eyes closed		
	Mean ± SD	Mean ± SD	t -Value	p -Value	
C_p	0.091 ± 0.005	0.086 ± 0.006	3.789	0.001	t1.6
L_p	0.327 ± 0.009	0.322 ± 0.009	1.953	0.064	t1.7
γ	0.382 ± 0.047	0.377 ± 0.049	0.372	0.714	t1.8
λ	0.185 ± 0.004	0.182 ± 0.004	2.544	0.019	t1.9
E_{loc}	0.123 ± 0.003	0.120 ± 0.004	4.112	0.000	t1.10
E_{glob}	0.090 ± 0.002	0.091 ± 0.002	-2.095	0.048	t1.11

Note: $C_p, L_p, \gamma, \lambda, E_{loc}$ and E_{glob} denote the clustering coefficient, characteristic path length, normalized clustering coefficient, normalized shortest path length, local efficiency, and global efficiency, respectively. Significant effects ($p < 0.05$) are indicated by bold text. With the Hirschberger–Qi–Steuer (H–Q–S) algorithm, the differences between eyes-open and eyes-closed in γ was significant ($t = 3.767, p = 0.001$) and in λ was not significant ($t = 1.206, p = 0.241$).

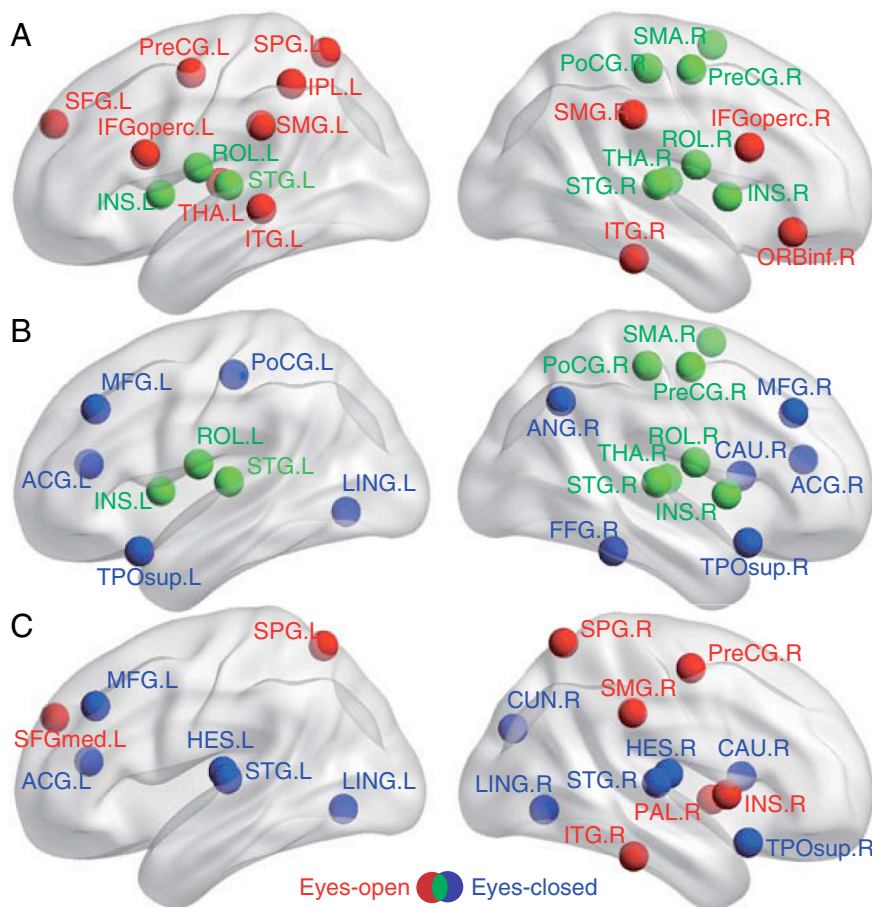


Fig. 3. Plots of nodal characteristics of functional neural networks rendered on the cortical surface. (A) Hub regions of the functional neural networks under eyes-open. The spheres in red indicate the hub regions specific to eyes-open, and those in green indicate the hub region shared in both eyes-open and eyes-closed. (B) Hub regions of the functional neural networks under eyes-closed. The spheres in blue indicate the hub regions specific to eyes-closed, and those in green indicate the hub region shared in both eyes-open and eyes-closed. (C) Brain regions showing significant differences in the integrated regional nodal parameters between eyes-open and eyes-closed. The spheres in red (blue) indicate the regions with significant higher (lower) value of nodal parameters (degree, or nodal efficiency, or betweenness centrality) under eyes-open compared with eyes-closed. The threshold was $p < 0.05$ (uncorrected). Nodes are mapped onto the cortical surfaces using BrainNet Viewer software (Xia et al., 2013).

340 Differences of nodal characteristics between EO and EC

341 Paired *t*-tests showed that eight brain regions exhibited significantly
 342 increased integrated nodal parameters (D , E_{nod} , or B) in the EO compared to EC ($p < 0.05$, uncorrected). These brain regions were mainly located in the oculomotor system (PreCG.R), attentional system (bilateral SPG) (Corbetta and Shulman, 2002; Fox et al., 2005, 2006), arousal system (INS.R) (Craig, 2009) and other regions such as ITG.R, SMG.R, SFGmed.L, and right pallidum (PAL.R) (red spheres, Fig. 3C; Table S3).
 347 Meanwhile, we also found that eleven brain regions showed significant
 348 increased integrated nodal parameters (D , E_{nod} , and BC) in EC compared
 349 to EO ($p < 0.05$, uncorrected). These brain regions were mainly involved
 350 with the visual system (bilateral LING, right cuneus (CUN.R)), auditory
 351 system (bilateral Heschl's gyrus (HES)) (Binder et al., 1994; Nobre
 352 et al., 1997), part of the default mode network (ACG.L) (Raichle et al.,
 353 2001; Van Dijk et al., 2010), and other regions (bilateral STG, CAU.R,
 354 MFG.L, and TPOsup.R) (blue spheres, Fig. 3C; Table S3).

356 Inter-regional functional connectivity

357 The network-based statistical method (NBS) revealed that 20 connections
 358 were significantly more correlated but 51 connections were significantly
 359 less correlated under EO than under EC (Fig. 4; Table S4). The one-tailed
 360 paired *t*-tests revealed three patterns of connectivity corresponding to
 361 EO > EC: positive correlations in both EO and EC, negative correlations
 362 in both EO and EC, positive correlations in EO but negative correlations
 363 in EC. Similar patterns were found in EO < EC by one-

tailed paired *t*-tests. Compared to EC, specifically, the more correlated
 364 connections under EO included seven increased positive connections,
 365 two decreased negative connections, and six connections positive in
 366 EO but negative in EC. These increased connections included five within
 367 the visual system and two between visual and attention systems. The
 368 two decreased negative connections were located between language
 369 and arousal systems, two between visual and subcortical regions, one
 370 between visual and language systems, and one between visual and emotion
 371 systems (Bechara et al., 2000). Additionally, the lower correlated
 372 connections under EO compared to EC included eleven decreased positive
 373 connections and forty negative connections in EO but positive in
 374 EC. The decreased positive connections included three between visual
 375 and somatosensory systems, five between visual and motor systems,
 376 two between visual and auditory systems (Celestia, 1976; Howard
 377 et al., 2000), and one between visual and language systems. The negative
 378 connections in EO but positive in EC included ten between visual and
 379 motor systems, thirteen between visual and somatosensory systems,
 380 thirteen between visual and auditory systems, and one between visual
 381 and language systems.

385 Discussion

386 Although previous studies have attempted to investigate different
 387 neural presentations of exteroceptive and interoceptive states by

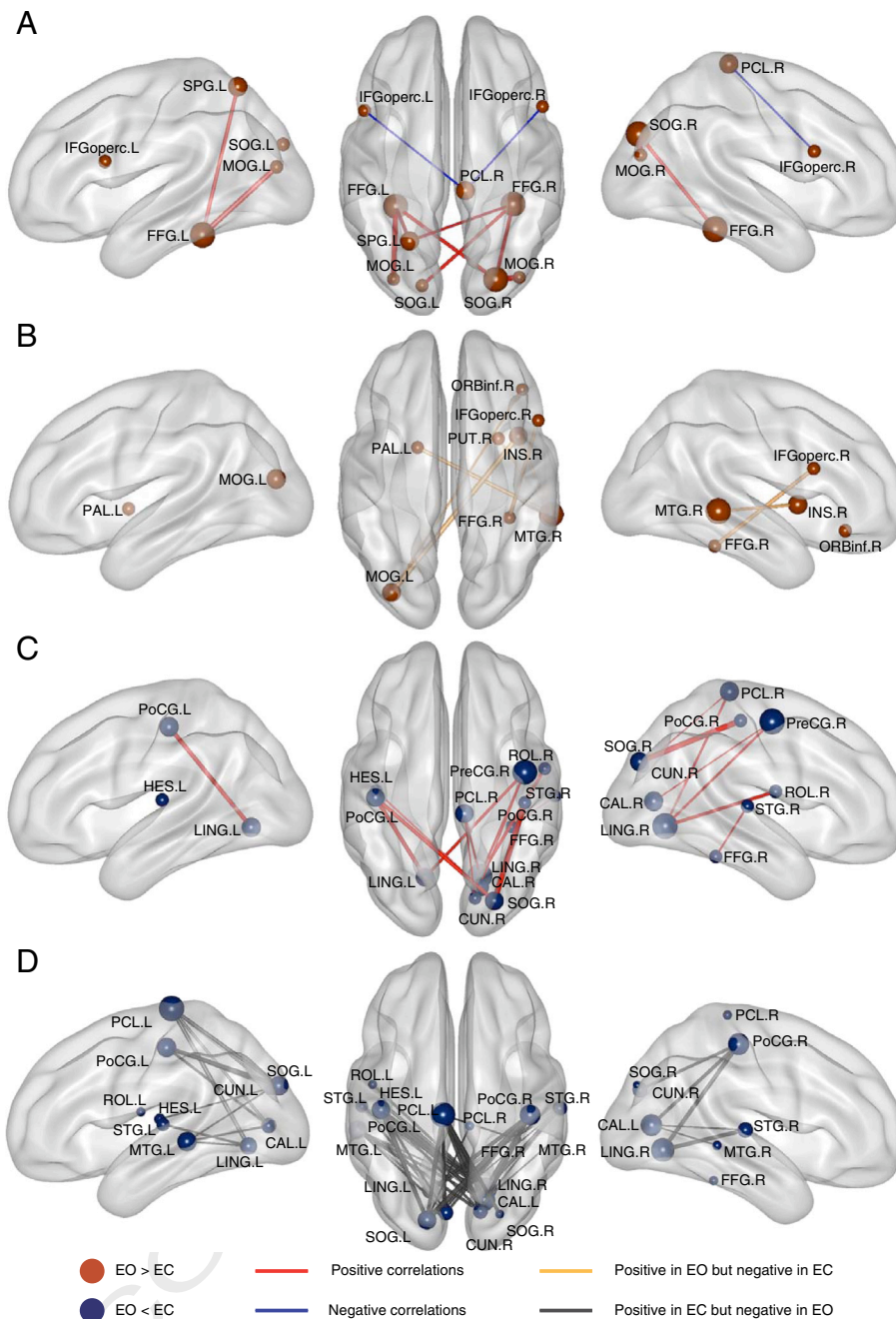


Fig. 4. Plots of the inter-regional functional connections showing significant differences between eyes-open (EO) and eyes-closed (EC). (A) EO > EC, positive (in red) and negative (in blue) correlations for EO compared to EC. (B) EO > EC, correlations that are positive in EO but negative in EC. (C) EO < EC, positive correlations in both EO and EC. (D) EO < EC, correlations that are negative in EO but positive in EC. The nodal size is proportional to the number of links of the node, and the line width was proportional to *t*-value of the connection. Nodes and connections are mapped onto the cortical surfaces using BrainNet Viewer software (Xia et al., 2013).

manipulating the orientation of attention (Farb et al., 2013; Simmons et al., in press), the easiest way to control the direction of visual attention that also balances task difficulty, is simply eyes opened versus eyes closed, an approach which has been largely overlooked. Although previous fMRI studies have found different influences of EO and EC on regional brain activity (Marx et al., 2003, 2004; Wiesmann et al., 2006; Yang et al., 2007) and functional connectivity (Van Dijk et al., 2010; Yan et al., 2009; Zou et al., 2009), the topological organizations of the whole brain networks and the corresponding information processing modes underlying these two states had not yet been identified.

Given that the small-world model supports both specialized and integrated information processing in the brain (Bassett and Bullmore,

2006; Sporns et al., 2004), we adopted graph theoretical approaches to investigate the organizations of brain networks under exteroceptive and interoceptive states with the manipulation of EO and EC. Our results showed that the brain functional networks for both EO and EC exhibited small-world properties, which supported recent findings of brain networks (for a review, see Wang et al., 2010). Thus, this study provided further evidence that functional brain networks exhibit robust small-world properties regardless of the selection of resting conditions, eyes-closed or eyes-open. More importantly, we provided evidence that the topological organizations corresponding to information processing modes of the human brain under the exteroceptive and interoceptive states are somewhat different; there are both domain-general

412 and domain-specific nodes. The domain-specific nodes seem to relate to
413 specialization of information processing and integration of information
414 processing.

415 *Increased specialized information processing in EO relative to decreased*
416 *integrated information processing in EC*

417 There are two major information processing modes in the functional
418 organization of the brain: specialized information processing and inte-
419 grated information processing, which serve to generate and integrate
420 information from external and internal sources, respectively (Friston,
421 2002; Tononi et al., 1998; Zeki and Shipp, 1988). Since information pro-
422 cessing occurs in real time (Sporns and Kötter, 2004), this study ex-
423 plored how the characteristic features and efficiency of the two
424 primary information processing modes might be altered if afferent visu-
425 al information was attenuated by closing the eyes.

426 Consistent with a previous R-MRI study which found higher regional
427 spontaneous activities in EO (Yan et al., 2009), our results showed
428 higher C_p and E_{loc} , which represents increased specialized information
429 processing when the eyes are open. This suggests that during EO,
430 non-specific or non-goal-directed information may be gathered and
431 evaluated in the brain automatically (Yan et al., 2009). Similar to previ-
432 ous findings of EEG desynchronization (Barry et al., 2007; Chen et al.,
433 2008), we also found higher λ and lower E_{glob} in EO, which indicated
434 the reduced integrated information processing of the functional net-
435 works. The connectivity findings further revealed that increased special-
436 ized information processing, but decreased integrated information
437 processing pattern in the EO, may result from more specific connections
438 within the visual system (such as MOG.R-SOG.R) and less connections
439 between systems (such as the connection between visual and somato-
440 sensory systems (e.g., LING-PreCG.R)) under EO relative to EC. The
441 efficiency of information processing under EC may be disturbed or sup-
442 pressed by EO (Niven and Laughlin, 2008), which reflects the higher
443 functional specialization of EO (Nir et al., 2006). Our findings demon-
444 strate that there is a modulation of increased specialized information
445 processing but decreased integrated information processing from EC
446 to EO, underlying the shift from interoceptive towards exteroceptive
447 state.

448 *Interoceptive network in EO and exteroceptive network in EC*

449 As previously proposed (Marx et al., 2003), there are two mental
450 states at opposite extremes of one another, an “exteroceptive” state
451 characterized by attention and oculomotor system activity under the
452 EO state, and an “interoceptive” state characterized by imagination and
453 multisensory integration under the EC state (Hufner et al., 2009; Marx
454 et al., 2004; Wiesmann et al., 2006). Our findings, which add evidence
455 based on the nodal properties of neural networks, further support this
456 proposition that there are two distinct networks underlying these two
457 states. One is the “exteroceptive” network, composed of the oculomotor
458 system (PreCG and SFG), attentional system (SPG and IPL) (Corbetta and
459 Shulman, 2002; Fox et al., 2005, 2006), and the arousal system (INS, ROL
460 and THA) (Critchley, 2004; Critchley et al., 2011). This network is specific
461 to EO, underlying the exteroceptive state for alertness and readiness
462 (Fransson, 2005; McAvoy et al., 2008). The other is the “interoceptive”
463 network, which mainly includes the visual system (LING., FFG, and
464 STG), auditory system (HES), somatosensory system (PoCG), and part
465 of the default mode network (ANG and ACG) (Raichle et al., 2001; Van
466 Dijk et al., 2010). This network is specific to EC, underlying introspective
467 state for imagination and recall of sensory experiences (Hufner et al.,
468 2009; Marx et al., 2003).

469 The present findings were consistent with previous investigations in
470 showing that both the activation of the visual system (mainly including
471 the extrastriate body area, such as LING) (Bianciardi et al., 2009; Hufner
472 et al., 2008, 2009; Marx et al., 2003, 2004) and the connections between
473 visual (mainly including the extrastriate body area) and motor system

(such as LING-PreCG.R) (Nir et al., 2006; Wiesmann et al., 2006; Zou
474 et al., 2009) are attenuated under EO compared to EC. Given that the
475 extrastriate body area (such as LING) and premotor cortex (such as
476 PreCG) are associated with body identity and body actions, respectively
477 (Astafiev et al., 2004; Downing et al., 2001; Urgesi et al., 2007), one pos-
478 sible interpretation is that the subjects were imagining body motion
479 during the suppression of natural urges in EC.
480

Cross-sensory modality connections are altered in EO/EC

481 Stronger coupling of the visual system with motor, somatosensory 482
and auditory system may indicate high synchronization across sensory 483
modalities during EC. Given that LING and FFG are believed to play an 484
important role in visual imagery and memory (Bogousslavsky et al., 485
1987; Machielsen et al., 2000), this higher coupling may be the result 486
of non-specific imagination leading to the recall of sensory experiences 487
during EC (Damasio, 1996; Marx et al., 2003). This cross-modality 488
synchronism was attenuated and the connections among visual and 489
attention, arousal, and subcortical systems were increased with eyes 490
opening; this may indicate that EO leads to a suppression of sensory mo- 491
dalities other than vision to capture more resources and energy for ex- 492
teroceptive processing (Bianciardi et al., 2009; Niven and Laughlin, 493
2008). These connectivity findings, consistent with network metrics, 494
further suggest a switch in information processing mode from highly inte- 495
grated (EC) to highly specialized (EO). 496

497 It is worth mentioning that a recent study reported no evidence of 498
differences in topological organization of brain functional networks be- 499
tween EO and EC (Jao et al., 2013). They did find widespread differences 500
between EO and EC on the spontaneous activity and functional connec- 501
tivity of brain, but there were no apparent differences on whole brain 502
topological organization other than the connection distance, an index 503
of the information processing of a network (Sepulcre et al., 2010), be- 504
tween EO and EC. Possible explanations for the discrepancy between 505
these two studies are as follows: (1) GSR was used in the present 506
study but not the previous one, (2) the parcellation templates were dif- 507
ferent, and (3) the spatial resolutions were different (data acquisition 508
parameters).

509 Global variations of the BOLD signal are often considered nuisance 510
effects and are commonly removed as a covariate in a regression 511
model. Thus, GSR is widely used to remove noise generated by the scan- 512
ner (such as signal drifting and spikes). There is much debate about its 513
utility in fMRI data pre-processing (Chai et al., 2012a; Fox et al., 2009; 514
Murphy et al., 2009; Weissenbacher et al., 2009), because it centers 515
the distribution of correlations around zero and may introduce spurious 516
correlations (Saad et al., 2012). The concern is especially relevant when 517
interpreting negative correlations, since they may be solely the result of 518
GSR, rather than reflecting true neuronal activation/deactivation 519
(Murphy et al., 2009). Though, it is worth noting that recent electro- 520
physiological work indicates wide-spread positive correlations across 521
nearly the entire cortex (Scholvinck et al., 2010). These wide-spread 522
correlations may require mitigation to examine local network proper- 523
ties. Additionally, recent work examining the impact of standardization 524
procedures (e.g., GSR and mean subtraction) for motion artifacts on 525
connectivity patterns, suggests that some normalization procedure 526
(e.g., GSR) is better than none (e.g., no GSR) (Yan et al., 2013) (PMID 527
23631983). Given these issues, we analyzed the data both with and 528
without GSR. Our results showed that differences in negative correla- 529
tions disappeared without GSR, but the pattern of main results and con- 530
clusion remained (Supplementary materials). Compared with results 531
without GSR, our results with GSR were more consistent with previous 532
results (Hufner et al., 2008; Marx et al., 2003, 2004; Nir et al., 2006; 533
Wiesmann et al., 2006). That is, our results with GSR were more sensi- 534
tive to the differences between EO and EC compared to those obtained 535
without GSR, which is also in consistent with the results of Fox et al. 536
(2009). Therefore, GSR is one possible reason for the discrepancy be- 537
tween our findings and those of Jao et al. (2013).

Given the important impact of different parcellation strategies (especially the spatial scale of the nodal parcellation) on topological parameters (e.g. small-worldness and efficiency) of functional brain networks (Power et al., 2011; Wang et al., 2009; Wig et al., 2011; Zalesky et al., 2010b), another potential explanation for the current discrepancy is the different parcellation templates. Although the topological parameters vary considerably as a function of spatial nodal scale (Zalesky et al., 2010b), it is hard to identify a specific nodal scale that maximize sensitivity to differences of topological organizations between conditions. For example, lower spatial resolution enhances signal-to-noise ratio of the time series at each region, which in turn adds noise to the inter-regional connectivity matrix. One possible explanation is that the sub-sampling of the anatomically based AAL template disturbs both intra- and inter-regional connections, which reduced the sensitivity to test the differences between EO and EC by Jao et al. (2013). Another explanation is that the higher spatial resolution in data acquisition increased the sensitivity in our study. These two possibilities are not mutually exclusive. Building on Jao et al.'s (2013) findings, the present study uses a more sensitive parcellation template and higher spatial resolution, which may further clarify the influence of volitional eye opening on the spontaneous activity of the brain. Taken together, volitional eye opening influences not only the spontaneous activity of the isolated brain regions and the inter-regional function connectivity, but also the functional integration of multiple brain regions and whole brain topological organizations.

Although EO and EC correspond to exteroceptive and interoceptive states respectively (Marx et al., 2003) and these correspondences are supported by both the current results and previous findings (Bianciardi et al., 2009; Brandt, 2006; Hufner et al., 2008, 2009; Marx et al., 2004; McAvoy et al., 2008, 2012; Niven and Laughlin, 2008), it potentially oversimplifies the relationship between EO/EC and exteroceptive/interoceptive states. We can neither argue that interoceptively oriented attention is absent under EO (Farb et al., 2013), nor that exteroceptively oriented attention is absent under EC (Fransson, 2005). More elaborate manipulations of attentional orientation should be conducted in the future to address this question (Farb et al., 2013; Simmons et al., in press). Since skin

conductance is a sensitive psychophysiological index of bodily state (Critchley, 2002; Critchley et al., 2004) and is highly correlated with spontaneous brain activity (Fan et al., 2012), skin conductance indices could shed further light on interoceptive and exteroceptive processing.

In summary, EO and EC were evaluated during resting state, without any top-down attentional manipulation, such as visual fixation (Bianciardi et al., 2009; Yang et al., 2007) or attentional orientation (Farb et al., 2013; Simmons et al., in press). Thus, the only differences between EO and EC were visual sensory information and subjective/objective state characteristics of EO and EC. Therefore, we speculate that the eyes act as a toggle between an exteroceptive network and interoceptive network rather than simply a gate of visual sensory information (Burton et al., 2004; Hufner et al., 2009). Having the eyes open or closed modulates a shift between prominently exteroceptive network activity and prominently interoceptive network activity, respectively. This shift, from EO to EC also corresponds to an information processing mode of more specialized towards more integrated. Taking into account the wide applicability of the R-fMRI and graph-based analysis to various studies, our findings also suggested that the choice of the resting condition (either eyes closed or eyes open) is an important factor to be carefully considered given different research objectives.

Acknowledgments

This work was supported by the Natural Science Foundation of China (Grant numbers: 81071149, 81030028, 81271548, and 81371535), National Science Fund for Distinguished Young Scholars (Grant number: 81225012), and Scientific Research Foundation for the Returned Overseas Chinese Scholars (RH), and State Education Ministry of China. We thank Alexander Dufford for offering helpful comments.

Conflict of interest

The authors declare no competing financial interests.

Appendix A

Table A
Expressions and descriptions of the network parameters applied in this study.

Network parameters	Definitions	Descriptions
Clustering coefficient (C_p)	$C_p = \frac{1}{N} \sum_{i \in G} \frac{K_i}{D(i)(D(i)-1)/2}$	C_p measures the local cliquishness of a network G with N nodes and K edges. K_i is the number of edges in $G(i)$, the subgraph consisting of the neighbors of node i .
Characteristic path length (L_p)	$L_p = \frac{1}{N(N-1)} \sum_{i \neq j \in G} \frac{1}{L_{ij}}$	L_p measures the overall routing efficiency of the network. L_{ij} is the shortest path length between nodes i and j .
Global efficiency (E_{glob})	$E_{glob} = \frac{1}{N(N-1)} \sum_{i \neq j \in G} \frac{1}{L_{ij}}$	E_{glob} measures the extent of information propagation through the whole network.
Local efficiency (E_{loc})	$E_{loc} = \frac{1}{N} \sum_{i \in G} E_{glob}(i)$	E_{loc} measures the mean local efficiency of the network.
Degree (D)	$D(i) = \sum_{j \neq i \in G} e_{ij}$	$D(i)$ measures the connectivity of node i with the rest of the nodes in a network, e_{ij} is the (i, j) th element in the formerly obtained binarized correlation matrix.
Efficiency (E_{nod})	$E_{nod}(i) = \frac{1}{N-1} \sum_{j \neq i \in G} \frac{1}{L_{ij}}$	$E_{nod}(i)$ measures the ability of information transmission of node i in the network.
Betweenness centrality (BC)	$BC(i) = \sum_{j \neq i, k \in G} \frac{\delta_{jk}(i)}{\delta_{jk}}$	$BC(i)$ measures the influence of node i over information flow between other nodes in the whole network. δ_{jk} is the number of the shortest paths from node j to node k , and $\delta_{jk}(i)$ is the number of the shortest paths from node j to node k that pass through node i within the network G .
Integrated global parameters (S_{glob})	$S_{glob} = \sum_{k=10}^{28} S(k \cdot \Delta s) \Delta s$	S_{glob} measures the area under curve (AUC) of each global network parameter ($C_p, L_p, \gamma, \lambda, E_{glob}$, and E_{loc}). $S(k \cdot \Delta s)$ represents any of the global parameters at the sparsity of $k \cdot \Delta s$, and Δs is the sparsity interval of 0.01. The range of sparsity was selected from 0.01 to 0.28 ($0.01 \leq k \leq 0.28$, see the Results section) in the current study.
Integrated nodal parameters (S_{nod})	$S_{nod}(i) = \sum_{k=10}^{28} S(i, k \Delta s) \Delta s$	S_{nod} measures the AUC of each nodal parameter (D, E_{nod} , and BC). $S(i, k \cdot \Delta s)$ represents any of the nodal parameters of the node i at a sparsity of $k \cdot \Delta s$.
Normalized nodal parameters (NS_{nod})	$NS_{nod}(i) = \frac{\sum_{k=1}^M S_{nod}(i, k)}{\sum_{j=1}^N \sum_{k=1}^M S_{nod}(j, k)}$	NS_{nod} is the normalized integrated nodal parameters. $S_{nod}(i, k)$ represents one of these three integrated nodal parameters (D, E_{nod} , and BC) at node i for the network of subject k ; N is the number of nodes and M is the number of subjects.
Hub identification criterion	$NS_{nod}(i) > \text{mean}(S) + SD$	The criterion to identify the hub. The mean (S) stands for the averaged value of $NS_{nod}(i)$, and SD for the standard deviation of $NS_{nod}(i)$ across all nodes of the network.

605 **Appendix B. Supplementary data**

606 Supplementary data to this article can be found online at <http://dx>.
607 doi.org/10.1016/j.neuroimage.2013.12.060.

608 **References**

- 609 Achard, S., Bullmore, E., 2007. Efficiency and cost of economical brain functional net-
610 works. *PLoS Comput. Biol.* 3, 174–183.
- 611 Astafiev, S.V., Stanley, C.M., Shulman, G.L., Corbetta, M., 2004. Extrastriate body area in
612 human occipital cortex responds to the performance of motor actions. *Nat. Neurosci.*
613 7, 542–548.
- 614 Barry, R.J., Clarke, A.R., Johnstone, S.J., Magee, C.A., Rushby, J.A., 2007. EEG differences
615 between eyes-closed and eyes-open resting conditions. *Clin. Neurophysiol.* 118,
616 2765–2773.
- 617 Bassett, D.S., Bullmore, E., 2006. Small-world brain networks. *Neuroscientist* 12, 512–523.
- 618 Bechara, A., Damasio, H., Damasio, A.R., 2000. Emotion, decision making and the
619 orbitofrontal cortex. *Cereb. Cortex* 10, 295–307.
- 620 Bianciardi, M., Fukunaga, M., van Gelderen, P., Horowitz, S.G., de Zwart, J.A., Duyn, J.H.,
621 2009. Modulation of spontaneous fMRI activity in human visual cortex by behavioral
622 state. *Neuroimage* 45, 160–168.
- 623 Binder, J.R., Rao, S.M., Hammeke, T.A., Yetkin, F.Z., Jesmanowicz, A., Bandettini, P.A., Wong,
624 E.C., Estkowski, L.D., Goldstein, M.D., Houghton, V.M., Hyde, J.S., 1994. Functional
625 magnetic-resonance-imaging of human auditory-cortex. *Ann. Neurol.* 35, 662–672.
- 626 Bogousslavsky, J., Miklossy, J., Deruaz, J.P., Assal, G., Regli, F., 1987. Lingual and fusiform gyri
627 in visual processing: a clinico-pathologic study of superior altitudinal hemianopia.
628 *J. Neurol. Neurosurg. Psychiatry* 50, 607–614.
- 629 Brandt, T., 2006. How to see what you are looking for in fMRI and PET – or the crucial
630 baseline condition. *J. Neurol.* 253, 551–555.
- 631 Bullmore, E., Sporns, O., 2009. Complex brain networks: graph theoretical analysis of
632 structural and functional systems. *Nat. Rev. Neurosci.* 10, 186–198.
- 633 Burton, H., Snyder, A.Z., Raichle, M.E., 2004. Default brain functionality in blind people.
634 *Proc. Natl. Acad. Sci. U. S. A.* 101, 15500–15505.
- 635 Celesia, G.G., 1976. Organization of auditory cortical areas in man. *Brain* 99, 403–414.
- 636 Chai, X.J., Castanon, A.N., Ongur, D., Whitfield-Gabrieli, S., 2012a. Anticorrelations in resting
637 state networks without global signal regression. *Neuroimage* 59, 1420–1428.
- 638 Chai, X.Q.J., Castanon, A.N., Ongur, D., Whitfield-Gabrieli, S., 2012b. Anticorrelations in
639 resting state networks without global signal regression. *Neuroimage* 59, 1420–1428.
- 640 Chen, A.C., Feng, W., Zhao, H., Yin, Y., Wang, P., 2008. EEG default mode network in the
641 human brain: spectral regional field powers. *Neuroimage* 41, 561–574.
- 642 Corbetta, M., Shulman, G.L., 2002. Control of goal-directed and stimulus-driven attention
643 in the brain. *Nat. Rev. Neurosci.* 3, 201–215.
- 644 Craig, A.D., 2009. How do you feel—now? The anterior insula and human awareness. *Nat.*
645 *Rev. Neurosci.* 10, 59–70.
- 646 Crick, F., Koch, C., 2003. A framework for consciousness. *Nat. Neurosci.* 6, 119–126.
- 647 Critchley, H.D., 2002. Electrodermal responses: what happens in the brain. *Neuroscientist*
648 8, 132–142.
- 649 Critchley, H.D., 2004. The human cortex responds to an interoceptive challenge. *Proc.*
650 *Natl. Acad. Sci. U. S. A.* 101, 6333–6334.
- 651 Critchley, H.D., Wiens, S., Rotshtein, P., Ohman, A., Dolan, R.J., 2004. Neural systems
652 supporting interoceptive awareness. *Nat. Neurosci.* 7, 189–195.
- 653 Critchley, H.D., Nagai, Y., Gray, M.A., Mathias, C.J., 2011. Dissecting axes of autonomic
654 control in humans: insights from neuroimaging. *Auton. Neurosci.* 161, 34–42.
- 655 Damasio, A.R., 1996. The somatic marker hypothesis and the possible functions of the
656 prefrontal cortex. *Philos. Trans. R. Soc. Lond. B Biol. Sci.* 351, 1413–1420.
- 657 Downing, P.E., Jiang, Y., Shuman, M., Kanwisher, N., 2001. A cortical area selective for
658 visual processing of the human body. *Science* 293, 2470–2473.
- 659 Fan, J., McCandliss, B.D., Fossella, J., Flombaum, J.L., Posner, M.I., 2005. The activation of
660 attentional networks. *Neuroimage* 26, 471–479.
- 661 Fan, J., Xu, P., Van Dam, N.T., Eilam-Stock, T., Gu, X., Luo, Y.J., Hof, P.R., 2012. Spontaneous
662 brain activity relates to autonomic arousal. *J. Neurosci.* 32, 11176–11186.
- 663 Farb, N.A., Segal, Z.V., Anderson, A.K., 2013. Attentional modulation of primary interoceptive
664 and exteroceptive cortices. *Cereb. Cortex* 23, 114–126.
- 665 Fox, P.T., Burton, H., Raichle, M.E., 1987. Mapping human somatosensory cortex with
666 positron emission tomography. *J. Neurosurg.* 67, 34–43.
- 667 Fox, M.D., Snyder, A.Z., Vincent, J.L., Corbetta, M., Van Essen, D.C., Raichle, M.E., 2005. The
668 human brain is intrinsically organized into dynamic, anticorrelated functional
669 networks. *Proc. Natl. Acad. Sci. U. S. A.* 102, 9673–9678.
- 670 Fox, M.D., Corbetta, M., Snyder, A.Z., Vincent, J.L., Raichle, M.E., 2006. Spontaneous neuronal
671 activity distinguishes human dorsal and ventral attention systems. *Proc. Natl.*
672 *Acad. Sci. U. S. A.* 103, 10046–10051.
- 673 Fox, M.D., Zhang, D., Snyder, A.Z., Raichle, M.E., 2009. The global signal and observed
674 anticorrelated resting state brain networks. *J. Neurophysiol.* 101, 3270–3283.
- 675 Fransson, P., 2005. Spontaneous low-frequency BOLD signal fluctuations: an fMRI investi-
676 gation of the resting-state default mode of brain function hypothesis. *Hum. Brain*
677 *Mapp.* 26, 15–29.
- 678 Freeman, L.C., 1977. A set of measures of centrality based on betweenness. *Sociometry* 40,
679 35–41.
- 680 Friederici, A.D., Ruschmeyer, S.A., Hahne, A., Fiebach, C.J., 2003. The role of left inferior
681 frontal and superior temporal cortex in sentence comprehension: localizing syntactic
682 and semantic processes. *Cereb. Cortex* 13, 170–177.
- 683 Friston, K., 2002. Beyond phrenology: what can neuroimaging tell us about distributed
684 circuitry? *Annu. Rev. Neurosci.* 25, 221–250.
- Griswold, M.A., Jakob, P.M., Heidemann, R.M., Nittka, M., Jellus, V., Wang, J., Kiefer, B.,
Haase, A., 2002. Generalized autocalibrating partially parallel acquisitions (GRAPPA).
Magn. Reson. Med. 47, 1202–1210.
- Hagmann, P., Cammoun, L., Gigandet, X., Meuli, R., Honey, C.J., Wedeen, V.J., Sporns, O.,
2008. Mapping the structural core of human cerebral cortex. *PLoS Biol.* 6, e159.
- He, Y., Evans, A., 2010. Graph theoretical modeling of brain connectivity. *Curr. Opin.*
Neurol. 23, 341–350.
- He, Y., Chen, Z., Evans, A., 2008. Structural insights into aberrant topological patterns of
large-scale cortical networks in Alzheimer's disease. *J. Neurosci.* 28, 4756–4766.
- Howard, M.A., Volkov, I.O., Mirsky, R., Garell, P.C., Noh, M.D., Granner, M., Damasio, H.,
Steinschneider, M., Reale, R.A., Hind, J.E., Brugge, J.F., 2000. Auditory cortex on the
human posterior superior temporal gyrus. *J. Comp. Neurol.* 416, 79–92.
- Hufner, K., Stephan, T., Glasauer, S., Kalla, R., Riedel, E., Deutschlander, A., Dera, T.,
Wiesmann, M., Strupp, M., Brandt, T., 2008. Differences in saccade-evoked brain acti-
vation patterns with eyes open or eyes closed in complete darkness. *Exp. Brain Res.*
186, 419–430.
- Hufner, K., Stephan, T., Flanagan, V.L., Deutschlander, A., Stein, A., Kalla, R., Dera, T., Fesl, G.,
Jahn, K., Strupp, M., Brandt, T., 2009. Differential effects of eyes open or
closed in darkness on brain activation patterns in blind subjects. *Neurosci. Lett.* 466,
30–34.
- Humphries, M.D., Gurney, K., Prescott, T.J., 2006. The brainstem reticular formation is a
small-world, not scale-free, network. *Proc. Biol. Sci.* 273, 503–511.
- Jao, T., Vertes, P.E., Alexander-Bloch, A.F., Tang, I.N., Yu, Y.C., Chen, J.H., Bullmore, E.T.,
2013. Volitional eyes opening perturbs brain dynamics and functional connectivity
regardless of light input. *Neuroimage* 69, 21–34.
- Latora, V., Marchiori, M., 2001. Efficient behavior of small-world networks. *Phys. Rev. Lett.*
710 87, 198701.
- Machielsen, W.C., Rombouts, S.A., Barkhof, F., Scheltens, P., Witter, M.P., 2000. fMRI of
visual encoding: reproducibility of activation. *Hum. Brain Mapp.* 9, 156–164.
- Marx, E., Stephan, T., Nolte, A., Deutschlander, A., Seelos, K.C., Dieterich, M., Brandt, T.,
2003. Eye closure in darkness animates sensory systems. *Neuroimage* 19, 924–934.
- Marx, E., Deutschlander, A., Stephan, T., Dieterich, M., Wiesmann, M., Brandt, T., 2004.
Eyes open and eyes closed as rest conditions: impact on brain activation patterns.
Neuroimage 21, 1818–1824.
- Maslov, S., Sneppen, K., 2002. Specificity and stability in topology of protein networks.
Science 296, 910–913.
- McAvoy, M., Larson-Prior, L., Nolan, T.S., Vaishnavi, S.N., Raichle, M.E., d'Avossa, G., 2008.
Resting states affect spontaneous BOLD oscillations in sensory and paralimbic cortex.
J. Neurophysiol. 100, 922–931.
- McAvoy, M., Larson-Prior, L., Ludwиков, M., Zhang, D., Snyder, A.Z., Gusnard, D.L., Raichle,
M.E., d'Avossa, G., 2012. Dissociated mean and functional connectivity BOLD signals
in visual cortex during eyes closed and fixation. *J. Neurophysiol.* 108, 2363–2372.
- Milo, R., Shen-Orr, S., Itzkovitz, S., Kashtan, N., Chklovskii, D., Alon, U., 2002. Network
motifs: simple building blocks of complex networks. *Science* 298, 824–827.
- Mowinckel, A.M., Espeseth, T., Westlye, L.T., 2012. Network-specific effects of age and in-
scanner subject motion: a resting-state fMRI study of 238 healthy adults. *Neuroimage*
63, 1364–1373.
- Murphy, K., Birn, R.M., Handwerker, D.A., Jones, T.B., Bandettini, P.A., 2009. The impact of
global signal regression on resting state correlations: are anti-correlated networks
introduced? *Neuroimage* 44, 893–905.
- Nakano, T., Kato, M., Morito, Y., Itoi, S., Kitazawa, S., 2013. Blink-related momentary acti-
vation of the default mode network while viewing videos. *Proc. Natl. Acad. Sci. U. S. A.*
110, 702–706.
- Newman, M.E.J., 2003. The structure and function of complex networks. *SIAM Rev.* 45,
167–256.
- Nir, Y., Hasson, U., Levy, I., Yeshurun, Y., Malach, R., 2006. Widespread functional connec-
tivity and fMRI fluctuations in human visual cortex in the absence of visual stimula-
tion. *Neuroimage* 30, 1313–1324.
- Niven, J.E., Laughlin, S.B., 2008. Energy limitation as a selective pressure on the evolution
of sensory systems. *J. Exp. Biol.* 111, 1792–1804.
- Nobre, A.C., Sebestyen, G.N., Gitelman, D.R., Mesulam, M.M., Frackowiak, R.S.J., Frith, C.D.,
1997. Functional localization of the system for visuospatial attention using positron
emission tomography. *Brain* 120, 515–533.
- Power, J.D., Cohen, A.L., Nelson, S.M., Wig, G.S., Barnes, K.A., Church, J.A., Vogel, A.C.,
Laumann, T.O., Miezin, F.M., Schlaggar, B.L., Petersen, S.E., 2011. Functional network
organization of the human brain. *Neuron* 72, 665–678.
- Power, J.D., Barnes, K.A., Snyder, A.Z., Schlaggar, B.L., Petersen, S.E., 2012. Spurious but
systematic correlations in functional connectivity MRI networks arise from subject
motion. *Neuroimage* 59, 2142–2154.
- Raichle, M.E., MacLeod, A.M., Snyder, A.Z., Powers, W.J., Gusnard, D.A., Shulman, G.L.,
2001. A default mode of brain function. *Proc. Natl. Acad. Sci. U. S. A.* 98, 676–682.
- Rizzolatti, G., Luppino, G., 2001. The cortical motor system. *Neuron* 31, 889–901.
- Rubinov, M., Sporns, O., 2010. Complex network measures of brain connectivity: uses and
interpretations. *Neuroimage* 52, 1059–1069.
- Saad, Z.S., Gotts, S.J., Murphy, K., Chen, G., Jo, H.J., Martin, A., Cox, R.W., 2012. Trouble at
rest: how correlation patterns and group differences become distorted after global
signal regression. *Brain Connect.* 2, 25–32.
- Satterthwaite, T.D., Wolf, D.H., Loughhead, J., Ruparel, K., Elliott, M.A., Hakonarson, H., Gur,
R.C., Gur, R.E., 2012. Impact of in-scanner head motion on multiple measures of func-
tional connectivity: relevance for studies of neurodevelopment in youth. *Neuroimage*
60, 623–632.
- Scholvinck, M.L., Maier, A., Ye, F.Q., Duyn, J.H., Leopold, D.A., 2010. Neural basis of global
resting-state fMRI activity. *Proc. Natl. Acad. Sci. U. S. A.* 107, 10238–10243.
- Sepulcre, J., Liu, H., Talukdar, T., Martincorena, I., Yeo, B.T., Buckner, R.L., 2010. The organi-
zation of local and distant functional connectivity in the human brain. *PLoS Comput.*
Biol. 6, e1000808.

- Q3 Simmons, W.K., Avery, J.A., Barcalow, J.C., Bodurka, J., Drevets, W.C., Bellgowan, P., 2014. Keeping the body in mind: insula functional organization and functional connectivity integrate interoceptive, exteroceptive, and emotional awareness. *Hum. Brain Mapp.* (in press). 772
- Sporns, O., Kötter, R., 2004. Motifs in brain networks. *PLoS Biol.* 2, e369. 773
- Sporns, O., Zwi, J.D., 2004. The small world of the cerebral cortex. *Neuroinformatics* 2, 145–162. 774
- Sporns, O., Chialvo, D.R., Kaiser, M., Hilgetag, C.C., 2004. Organization, development and function of complex brain networks. *Trends Cogn. Sci.* 8, 418–425. 775
- Tian, L., Wang, J., Yan, C., He, Y., 2011. Hemisphere- and gender-related differences in small-world brain networks: a resting-state functional MRI study. *Neuroimage* 54, 191–202. 776
- Tononi, G., Edelman, G.M., Sporns, O., 1998. Complexity and coherency: integrating information in the brain. *Trends Cogn. Sci.* 2, 474–484. 777
- Tzourio-Mazoyer, N., Landeau, B., Papathanassiou, D., Crivello, F., Etard, O., Delcroix, N., Mazoyer, B., Joliot, M., 2002. Automated anatomical labeling of activations in SPM using a macroscopic anatomical parcellation of the MNI MRI single-subject brain. *Neuroimage* 15, 273–289. 778
- Urgesi, C., Candidi, M., Ionta, S., Aglioti, S.M., 2007. Representation of body identity and body actions in extrastriate body area and ventral premotor cortex. *Nat. Neurosci.* 10, 30–31. 779
- Van Dijk, K.R., Hedden, T., Venkataraman, A., Evans, K.C., Lazar, S.W., Buckner, R.L., 2010. Intrinsic functional connectivity as a tool for human connectomics: theory, properties, and optimization. *J. Neurophysiol.* 103, 297–321. 780
- Van Dijk, K.R., Sabuncu, M.R., Buckner, R.L., 2012. The influence of head motion on intrinsic functional connectivity MRI. *Neuroimage* 59, 431–438. 781
- Van Essen, D.C., 1979. Visual areas of the mammalian cerebral cortex. *Annu. Rev. Neurosci.* 2, 227–263. 782
- Wang, J., Wang, L., Zang, Y., Yang, H., Tang, H., Gong, Q., Chen, Z., Zhu, C., He, Y., 2009. Parcellation-dependent small-world brain functional networks: a resting-state fMRI study. *Hum. Brain Mapp.* 30, 1511–1523. 783
- Wang, J., Zuo, X., He, Y., 2010. Graph-based network analysis of resting-state functional MRI. *Front. Syst. Neurosci.* 4, 16. 784
- Watts, D.J., Strogatz, S.H., 1998a. Collective dynamics of 'small-world' networks. *Nature* 393, 440–442. 785
- Watts, D.J., Strogatz, S.H., 1998b. Collective dynamics of 'small-world' networks. *Nature* 393, 440–442. 786
- Weissenbacher, A., Kasess, C., Gerstl, F., Lanzenberger, R., Moser, E., Windischberger, C., 2009. Correlations and anticorrelations in resting-state functional connectivity MRI: a quantitative comparison of preprocessing strategies. *Neuroimage* 47, 1408–1416. 808
- Wiesmann, M., Kopietz, R., Albrecht, J., Linn, J., Reime, U., Kara, E., Pollatos, O., Sakar, V., Anzinger, A., Fesl, G., Bruckmann, H., Kobal, G., Stephan, T., 2006. Eye closure in darkness animates olfactory and gustatory cortical areas. *Neuroimage* 32, 293–300. 809
- Wig, G.S., Schlaggar, B.L., Petersen, S.E., 2011. Concepts and principles in the analysis of brain networks. *Ann. N. Y. Acad. Sci.* 1224, 126–146. 810
- Xia, M., Wang, J., He, Y., 2013. BrainNet Viewer: a network visualization tool for human brain connectomics. *PLoS One* 8, e68910. 811
- Yan, C.-G., Zang, Y.-F., 2010. DPARSF: a MATLAB toolbox for "pipeline" data analysis of resting-state fMRI. *Front. Syst. Neurosci.* 4, 13. 812
- Yan, C., Liu, D., He, Y., Zou, Q., Zhu, C., Zuo, X., Long, X., Zang, Y., 2009. Spontaneous brain activity in the default mode network is sensitive to different resting-state conditions with limited cognitive load. *PLoS One* 4, e5743. 813
- Yan, C.G., Craddock, R.C., Zuo, X.N., Zang, Y.F., Milham, M.P., 2013. Standardizing the intrinsic brain: towards robust measurement of inter-individual variation in 1000 functional connectomes. *Neuroimage*. 814
- Yang, H., Long, X.Y., Yang, Y., Yan, H., Zhu, C.Z., Zhou, X.P., Zang, Y.F., Gong, Q.Y., 2007. Amplitude of low frequency fluctuation within visual areas revealed by resting-state functional MRI. *Neuroimage* 36, 144–152. 815
- Zalesky, A., Fornito, A., Bullmore, E.T., 2010a. Network-based statistic: identifying differences in brain networks. *Neuroimage* 53, 1197–1207. 816
- Zalesky, A., Fornito, A., Harding, I.H., Cocchi, L., Yucel, M., Pantelis, C., Bullmore, E.T., 2010b. Whole-brain anatomical networks: does the choice of nodes matter? *Neuroimage* 50, 970–983. 817
- Zalesky, A., Fornito, A., Bullmore, E., 2012. On the use of correlation as a measure of network connectivity. *Neuroimage* 60, 2096–2106. 818
- Zeki, S., Shipp, S., 1988. The functional logic of cortical connections. *Nature* 335, 311–317. 819
- Zou, Q., Long, X., Zuo, X., Yan, C., Zhu, C., Yang, Y., Liu, D., He, Y., Zang, Y., 2009. Functional connectivity between the thalamus and visual cortex under eyes closed and eyes open conditions: a resting-state fMRI study. *Hum. Brain Mapp.* 30, 3066–3078. 820
- Zuo, X.N., Xu, T., Jiang, L., Yang, Z., Cao, X.Y., He, Y., Zang, Y.F., Castellanos, F.X., Milham, M.P., 2013. Toward reliable characterization of functional homogeneity in the human brain: preprocessing, scan duration, imaging resolution and computational space. *Neuroimage* 65, 374–386. 821